Scientific African 17 (2022) e01340

Contents lists available at ScienceDirect

Scientific African

journal homepage: www.elsevier.com/locate/sciaf

Enrichment of lead and cadmium from water using $P-ZrO_2CeO_2ZnO$ nanoparticles/alginate beads: Optimization and determination of significant factors and interaction using response surface methodologies

Nichodimus Hokonya[a,*], Courtie Mahamadi Prof, PhD[a,d], Netai Mukaratirwa-Muchanyereyi, PhD[a], Timothy Gutu, PhD[b], Caliphs Zvinowanda[c]

[a] Department of Chemistry, Bindura University of Science Education, P. Bag 1020 Bindura, Zimbabwe
[b] Department of Physics, University of Zimbabwe, P.O. Box MP 167 Mount Pleasant Harare, Zimbabwe
[c] Department of Chemical Sciences, Faculty of Science, University of Johannesburg, Doornfontein Campus, P.O Box 17011, Johannesburg, 2028, Republic of South Africa
[d] Director-Research and Postgraduate Centre, Bindura University of Science Education, P Bag 1020 Bindura, Zimbabwe

ARTICLE INFO

Article history:
Received 8 June 2022
Revised 1 August 2022
Accepted 23 August 2022

Handling Editor DR B Gyampoh

Keywords:
Solid phase extraction
Variables
Taguchi design
Half factorial design
Lead
Cadmium
Nanoparticles
Response surface methodology

ABSTRACT

The optimization, determination of significant factors and interactions between factors of the solid phase extraction method for the enrichment of lead and cadmium in water using $P-ZrO_2CeO_2ZnO$ nanoparticles/alginate beads was evaluated using Half factorial and Taguchi designs as response surface methodologies in this study. *Methods.* The beads were characterized using Fourier Transform Infra-Red spectroscopy, Brunauer-Emmet-Teller analysis, Scanning Electron Microscopy and Powder X-ray Diffraction. The amount of adsorbent (50, 100, 150 mg), sample volume (10, 50, 100 mL), eluent volume (10 mL), sample pH (3, 6, 9), eluent concentration (0.5, 1.0 and 2.0 M) and sample flow rate 2 rpm and eluent flow 3 rpm were used during the optimization experiments. The Half factorial design was used to screen for the most significant variables and the Taguchi design was then used to optimize the screened significant variables. *Findings* The sample volume was the most significant variable for cadmium recovery at $p = 0.05$. Interactions were noted between sample volume and sorbent dosage, sample volume and pH as well as sorbent dosage and pH. The method was validated by spiking cadmium and lead into borehole and well water samples. The recoveries for metal ions ranged from 57.0 -147.70% for cadmium and 33.12–116.5% for *lead*, limits of detection were 0.0297 ng/L for cadmium and 0.1022 ng/L for *lead*. This method exhibits potential for the enrichment of lead and cadmium from water samples.

* Corresponding author.
E-mail addresses: hokonyanichodimus@gmail.com (N. Hokonya), cmahamadi@buse.ac.zw (C. Mahamadi Prof), nmuchanyereyi@buse.ac.zw (N. Mukaratirwa-Muchanyereyi), tgutu@science.uz.ac.zw (T. Gutu).

https://doi.org/10.1016/j.sciaf.2022.e01340

Introduction

Potentially toxic elements are non-biodegradable, aggregate and stable compounds which pollute the environment. Asernic, cadmium, chromium, mercury, nickel, and lead are the most dangerous metals which are potentially toxic elements [21]. Cadmium is a non-essential metal which is highly toxic at very low exposure levels. It is released into the environment through forest fires, volcanic eruptions, sea sprays, welding, mining, cigarette smoking and refineries [23]. It has a wide range of toxicities on respiratory, renal and nervous systems. Cadmium is also said to be carcinogenic in large doses [17,9]. The maximum permissible limit for cadmium in drinking water according to WHO guidelines is 0.003 mg/L. Lead is highly toxic at low concentration. Long-term exposure of the body to lead at low concentration results in accumulation due to its low rate of excretion. Lead accumulation in the body can cause blood and brain disorders as well as serious nervous system disorders [9]. The maximum permissible limit of lead in drinking water according to WHO guideline is 0.01 mg/L [42].The concentration of cadmium and lead in the majority of samples is usually around the detection limit of the most sensitive analytical techniques. Accurate determination of these metals is a very important goal for analytical chemists, hence the aim of most researchers is to improve the analytical potential of the different analytical techniques [25]. Cadmium and lead has been determined quantitatively using Voltammetry [18], Electrothermal Atomic Adsorption Spectrometry (ETAAS) [37], Square Wave Anodic Stripping Voltammetry (SWASV) [4,24], Inductively Coupled Plasma Mass Spectrometry (ICP-MS) [28], High Resolution Continuum Source Graphite Furnace Atomic Absorption Spectrometry [47], Anodic Stripping Voltammetry [19], Flowing Liquid Anode Atmospheric Pressure Glow Discharge OES [12] among other methods. ICP-MS is the most powerful method due to its wide dynamic linear range, low limits of detection, multielement/isotope analysis capability and little mass interference. However, the application of ICP-MS for direct trace and ultra-trace metal analysis suffers from matrix effects and in some cases the target metal concentration is lower than the instrument detection limits. Hence the appropriate sample pre-treatment process is necessary prior to ICP-MS detection for the enrichment of target elements and removal of interfering sample matrix [16]. Lead and cadmium has been enriched using Solid Phase Extraction [8], Reverse Phase Dispersive Liquid- Liquid Microextration [35,29], Ultrasound-Assisted Surfactant Enhanced Emulsification Microextration [44], Liquid Phase Microextration [22], Mixed Cloud Point/Solid Phase Extraction [31]. Solid phase extraction is the ideal method for sample preparation since it involves enrichment, extraction and clean up procedures being performed in simple multiple steps. The advantages of micro solid phase extraction include low sample consumption, high concentration factors, excellent reproducibility, simplicity of operation and short extraction time [11,36]. One of the most challenging parts of solid phase extraction is the development of innovative micro-extraction sorbents which meets many requirements such as selectivity, stability, low costs, repeated use and versatility [15].

Many studies have employed one-factor at a time (OFAT) method to determine the sample sizes and testing procedures, regardless the economic issues and the weakness of this method in examining interaction effects of variables. The shortcomings of OFAT can be overcome by using Response surface methodology (RSM) which is comprised of statistical procedures applied to determine the optimum conditions for experimental conditions by considering the lowest numbers of experiments. The advantages of RSM are minimal numbers of experiments, less chemicals are consumed and less cost [3].The RSM also generate mathematical models that permits the assessments of the relevant interaction effects and statistical significance of factors [32]. The Taguchi experimental design is based on the application of orthogonal arrays which are employed to minimize the number of experiments to be performed and they are useful for identifying the effect and the importance of the factors on the response variable of the experimental design [39].

Considering the benefits of RSM and also that no study was carried out for enrichment of cadmium and lead using novel $P-ZrO_2CeO_2ZnO$ nanoparticles/alginate beads the objectives of the study were as follows; i) synthesis and characterization of $P-ZrO_2CeO_2ZnO$ nanoparticles/alginate beads ii) optimization of the enrichment process using the Taguchi experimental design iii) determination of significant factors and interaction between factors such as the amount of adsorbent, sample volume, eluent volume, sample pH and eluent concentration.

Materials and methods

Materials

The chemicals and reagents used in this study were analytical grade and utilized as received without further purification. Zirconyl chloride octahydrate 99.5% (Riedel-De-Haen, AG), zinc nitrate hexahydrate 99.5% (Merck, RSA), cerium sulphate tetra hydrate 98% (Merck, RSA) cadmium chloride hydrate (Sarchem, RSA), lead nitrate (Skylab's, SA), phenol (91%) (Riedel-de-Haen, AG), methanol (Avonchem, UK), propan-2-ol (ACE, RSA), phosphoric acid (Merck, RSA), sodium hydroxide (Glassworld, RSA), hydrochloric acid, nitric acid (Merck, RSA), calcium chloride (Merck, RSA) sodium alginate (Sigma Aldrich USA), were used throughout the study.

Preparation of $P-ZrO_2CeO_2ZnO$ *nanoparticles/alginate beads*

The $P-ZrO_2CeO_2ZnO$ nanoparticles were prepared by mixing 0.05 M Zirconium oxide chloride 8 hydrate, 0.05 M Cerium sulfate tetra hydrate, 0.05 M Zinc nitrate hexahydrate and an aqueous extract of *Flacourtia indica* plant leaves which acted as the reducing agent. The metal salt to plant extract ratio was 1:4 at pH 9.0 and the metal ion plant mixture was heated until

the colour changed from brown to beige to brown again upon production of $P-ZrO_2CeO_2ZnO$ nanoparticles. The nanoparticles were recovered using centrifugation at 5000 rpm followed by oven drying at 100 °C . The nanoparticles were calcined in a muffle furnace (Carbolite, England) at 900 °C for 3 h. The alginate beads were produced by mixing 100 mL of 2% w/v sodium alginate with 1 g of $P-ZrO_2CeO_2ZnO$ nanoparticles using a magnetic stirrer (Stuart Scientific), for four hours and the mixture was dropped into 1 M calcium chloride using a burette to form 1%, $P-ZrO_2CeO_2ZnO$ nanoparticle/alginate beads. The beads which formed were cured in 2 M calcium chloride solution for 12 h at room temperature. The obtained $P-ZrO_2CeO_2ZnO$ nanoparticle /alginate beads, were oven (Biobase, China) dried at 100 °C for 12 h to induce shrinking.

Characterisation of the $P-ZrO_2CeO_2ZnO$ *nanoparticles/alginate beads*

The functional groups responsible for enrichment of the metal ions were characterised using an Attenuated Total Reflectance Fourier Transform –Infra Red Spectrometer (ATR-FTIR) (Thermo-fisher scientific) operated at an average of 16 scans, a resolution of 2 cm^{-1} and scanning from 4000- 400 cm^{-1}. The beads were dried after enrichment reactions before being subjected to FTIR analysis. A D2 Phaser Powder X-Ray Diffraction (P-XRD) (Bruker, Germany), was used to determine the crystallinity of the beads with Cu K ($\propto$=1.5406) radiation. The scanning mode used was continuous with a scanning range 2 θ from 10 – 90 ° Samples were ground into fine powder and placed on sample holder. The surface area was also determined by BET surface area analysis. A 300 mg quantity of the beads was used for analysis. Relevant information was obtained as follows. A plot of pore size versus incremental pore volume gave pore size distribution. A plot of pore size versus pore volume gave total pore volume. The surface areas and total pore volumes of the beads were also obtained. The size of the nanoparticles was determined using a Transmission Electron Microscope (TEM) (Tecnai F20, FEI USA) operated at an accelerating voltage of 200 kV. The morphology and shape of the beads was characterized using a Scanning Electron Microscope (SEM, Zeiss Auriga Germany) at an accelerating voltage of 200 V. The beads were deposited on electron microscopy grids operated at an accelerated voltage of 200 V with scanning mode and observed. For the determination of the metals concentration in $P-ZrO_2CeO_2ZnO$ nanoparticles/alginate beads, a weighed amount of the beads was dissolved in 20 mL of 1 M nitric acid /hydrochloric acid and boiled until minimum volume was left. The sample was toped up to 25 mL using deionized water and filtered before analysis using Inductively Coupled Mass Spectrometer (ICP-MS 7900) (Agilent, Australia).

Syringe solid phase extraction procedure

Glass wool was used to cover the bottom of the 5 mL syringe and a weighed amount of $P-ZrO_2CeO_2ZnO$ nanoparticle/alginate beads was loaded and covered with glass wool. The beads and glass wool were prewashed using 0.1 M nitric acid and deionized water before loading the sample. A peristaltic pump (Eyela, Japan) was used to drive the solutions through the syringe column. A model solution consisting of 10 µg/L of lead and cadmium was prepared using deionized water and the pH was adjusted using 0.1 M nitric acid and 0.1 M sodium hydroxide. The pH of the model solution was monitored using a pH meter (Adwa AD1020-Romania). In this study a Half Factorial Design experimental design was used as a screening step to determine the significant variables. The Taguchi design was used to optimize of the significant variables. The amount of adsorbent (50, 100, 150 mg), sample volume (10, 50, 100 mL), eluent volume (10 mL), sample pH (3, 6, 9), eluent concentration (0.5, 1.0 and 2.0 M) and sample flow rate 2 rpm and eluent flow 3 rpm were used during the optimization experiments. Recovery studies using real samples were used to assess the extraction efficiency from the syringe column. The retained metals were eluted using nitric acid from the syringe column and diluted in a ratio of 1 mL of eluted sample to 10 mL of nitric acid prior to ICP-MS analysis. [46]. Each experiment was repeated twice to obtain reproducible results. ANOVA was used to determine the effect of parameters on sorption. The optimum eluent concentration was investigated by passing 10 mL of 0.5, 1.0, 2.0 M nitric acid through the loaded column and the one with the highest desorption was used as the eluting acid. For adsorption/desorption studies, the adsorbent was washed using nitric acid before being used again for a new cycle of extraction. The Extraction recovery (ER%) was used to investigate the effect of desorption conditions on the release of the metals from the surface of the beads. The optimized procedure was applied for the recovery of cadmium and lead from spiked well and borehole water samples. The water samples were collected in clean plastic containers followed by filtration using a 0.45 µm filter paper and acidified using 1 M nitric acid. The water samples were stored at 4 °C prior to analysis.

The Extraction recovery (ER%) was determined using the ratio of eluted concentration to the initial concentration as shown in Eq. (1),

$$ER\ \% = \frac{C_{des}\ X\ V_{des}}{C_0\ X\ V_0}\ X\ 100 \quad (1)$$

Where C_{des}, C_0, C_{des}, V_{des} *and* $V_0$are the analyte concentration in the extraction solvent, analyte concentration in the sample, extraction solvent volume and sample volume.

Adsorption studies

The adsorption capacity of $P-ZrO_2CeO_2ZnO$ nanoparticles/alginate beads was determined using batch studies on an orbital shaker. Equilibrium adsorption experiments were carried out with initial concentration ranging from 10 to 100 mg/L,

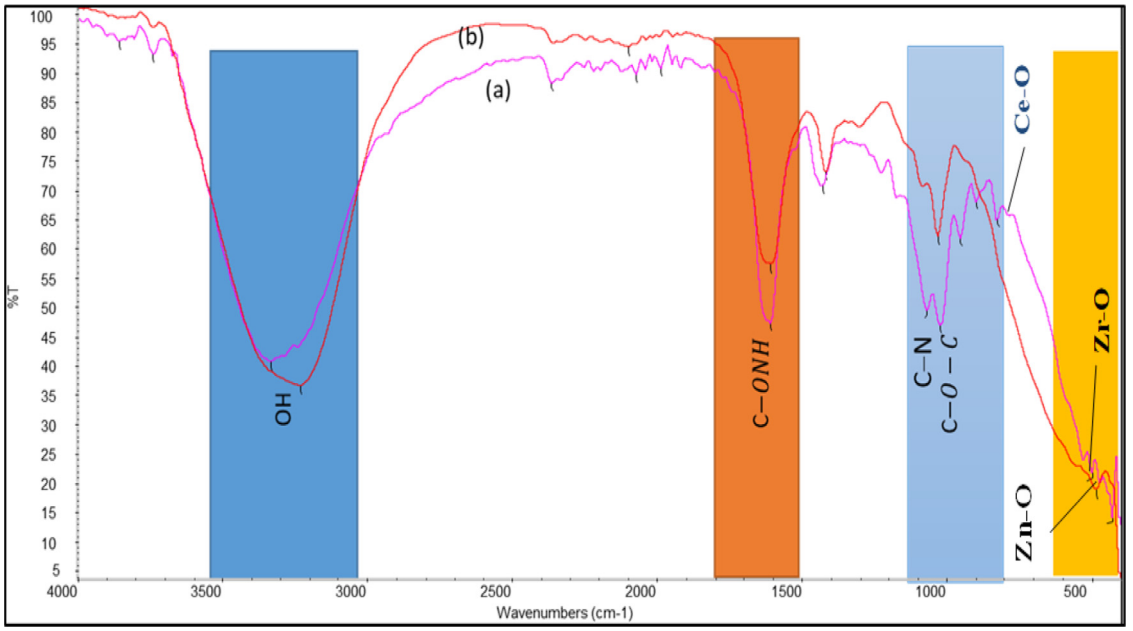

Fig. 1. The FT IR spectrum of a $P-ZrO_2CeO_2ZnO$ nanoparticles/alginate composite a) before and b) after enrichment.

dosage 150 mg, volume 100 mL and pH 7. The solutions were filtered using a 0.45 µm filter paper after reaching equilibrium and quantified using an ICP-MS spectrometer. The adsorption capacity at different concentrations was determined using the Eq. (2),

$$q_e = \frac{(C_o - C_e)}{m} \quad (2)$$

Where q_e is the adsorption equilibrium capacity (mg/g), v is the solution volume (L), m is the amount of the $P-ZrO_2CeO_2ZnO$ nanoparticles/alginate beads in grams, C_o and C_e are the initial and equilibrium concentration of cadmium and lead in mg/L.

Result and discussion

The FT-IR spectrum of $P-ZrO_2CeO_2ZnO$ nanoparticles/alginate beads before and after sorption is shown in Fig. 1. The spectrum of 1 % $P-ZrO_2CeO_2ZnO$ nanoparticle/ alginate beads (Fig. 1a) shows an "$O-H$ band", at 3332 cm^{-1} [30,2], "C – O stretching of amide", at 1601 cm^{-1}, "C – N stretching of amines at 1127 cm^{-1} [20] and a "C – O – C saccharide stretching", of alginate at 1061 and 1018 cm^{-1} [10]. After sorption (Fig. 1 b) the "$O-H$ band", shifts to 3231 cm^{-1}, "C – O group" remained at 1601 cm^{-1}, "C – N group", shift to 1111 cm^{-1} and the "C – O – C group", shifts to 1027 cm^{-1} . The vibration bands of nanoparticles Ce-O-C at 712 cm^{-1} [6], Zn-O stretching mode at 508 cm^{-1} [13] and Zr-O at 493 cm^{-1} [14,7] were totally absent after sorption. The bands which shifted or were totally absents was due to interactions between lead and cadmium with the sorbent indicating that the groups which shifted may have participated in enrichment on a minor scale.

The BET surface area of the $P-ZrO_2CeO_2ZnO$ nanoparticles/alginate beds was determined using BET N_2 adsorption-desorption isotherms. Inclusion of the "$P-ZrO_2CeO_2ZnO$ nanoparticles", into the calcium alginate beads increased their surface area from 4.38 to 7.33 m^2g^{-1}, micropore area from 0.51 to 3.82 m^2g^{-1}, and external surface area from 0.34 to 3.50 m^2g^{-1} .

The size of the "$P-ZrO_2CeO_2ZnO$ nanoparticles", was determined by Transmission Electron Microscopy imaging as shown in Fig. 2a) and b) and they ranged from 0.1 - 4.53 nm. The average nanoparticle particle size was 0.25 nm. The shape of the nanoparticles was irregular to cubic in morphology. The morphology of "$P-ZrO_2CeO_2ZnO$ nanoparticles/alginate beads", was determined using Scanning Electron Microscopy as shown in Fig. 2c) and the nanoparticles within the alginate beads were found to be cubic in shape with clusters in some places. The crystallinity of the of $P-ZrO_2CeO_2ZnO$ nanoparticles/alginate beads was determined using a D2-Phaser Powder X-ray Diffractometer. The diffraction pattern of the beads is shown in Fig. 2d and the pattern suggests that the material is amorphous. This suggested that the nanoparticles did not retain their original structure. The nanoparticle structure was disturbed by the polymeric alginate structure.

The amount of metals incorporated into the nanoparticles and nanoparticles encapsulated into alginate were determined by ICP-MS. The results show that the nanoparticles were successfully incorporated in the alginate beads. The amount of zinc, zirconium and cerium in mg/g were 6363.2, 3458.48 and 2957.64 in $P-ZrO_2CeO_2ZnO$ nanoparticles and 622.73, 360.74 and 395.14 in 1% $P-ZrO_2CeO_2ZnO$ nanoparticle/alginate beads respectively.

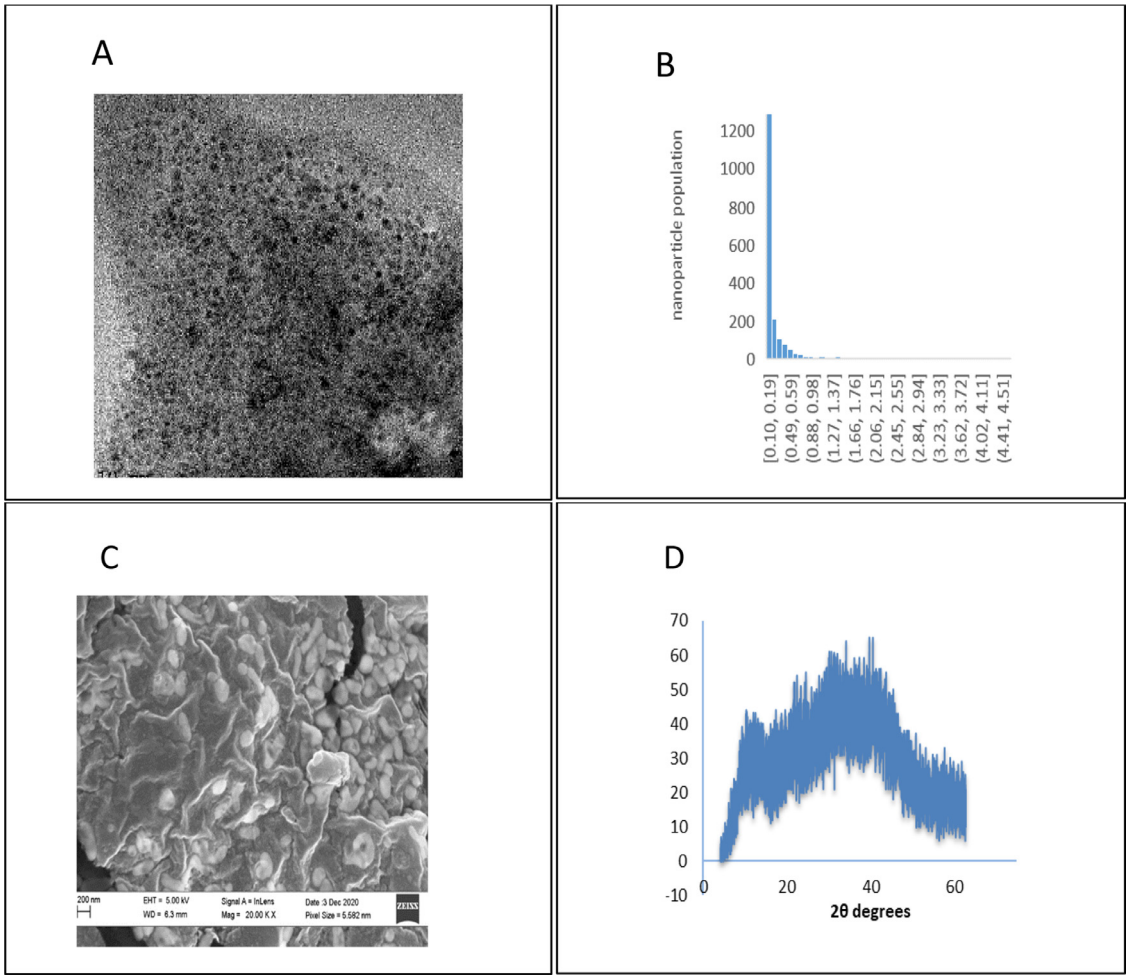

Fig. 2. a) TEM image, b) particle size distribution of $P-ZrO_2CeO_2ZnO$ nanoparticles c) SEM image of $P-ZrO_2CeO_2ZnO$ nanoparticles/alginate beads d) The XRD pattern of $P-ZrO_2CeO_2ZnO$ nanoparticles/alginate beads.

Table 1a
Langmuir, Freundlich, D-R and *Temkin* isotherm parameters.

	Langmuir			Freundlich					D-R		Temkin		
	Q (mg/g)	B (L/mg)	R	KF (mg/g)	n	R	Xm (mg/g)	K_{DL} Mol^2/J^2	E (KJ/mol)	R	K_T (L/g)	B J/mol	*R*
Cd	1.277	−0.045	0.953	0.618	0.749	0.985	62.89	4.28	0.34	0.99	−35.2	24.01	0.97
lead	0.13	−0.011	0.94	8.861	0.89	0.975	292.93	−0.015	0.12	0.96	8.39	27.67	0.93

The *Langmuir, Freundlich, Temkin* and *Dubinin Radushkevich* isotherm model parameters are shown in Table 1a.

Adsorption equilibrium studies

The performance of a sorbent in enrichment studies was evaluated by determining the adsorption capacity which establishes how much sorbent is required to quantitatively concentrate the metals from aqueous matrices. The adsorption equilibrium studies were determined by varying the *Cd* and *lead* concentration from 10 - 100 mg/L, the sample volume was kept at 100 mL, the optimum pH was 7, the adsorbent dosage was 150 mg of $P-ZrO_2CeO_2ZnO$ nanoparticle/alginate beads. The maximum adsorption capacity was determined by fitting the adsorption data into *Freundlich, Langmuir, Temkin and Dubinin Radushkevich* models (See Table 1a). The fitness of the isotherms was judged using the correlation coefficient R^2. The maximum adsorption capacity was 62.89 mg/g for cadmium and 292.93 mg/g for lead according to the *Dubinin Radushkevich* equation. *Cd* fitted the *Dubinin Radushkevich* equation with $R = 0.992$ and represented by Eq. (3),

$$ln\, q_e = ln\, 4.26 + 0.068\, \varepsilon 2 \quad (3)$$

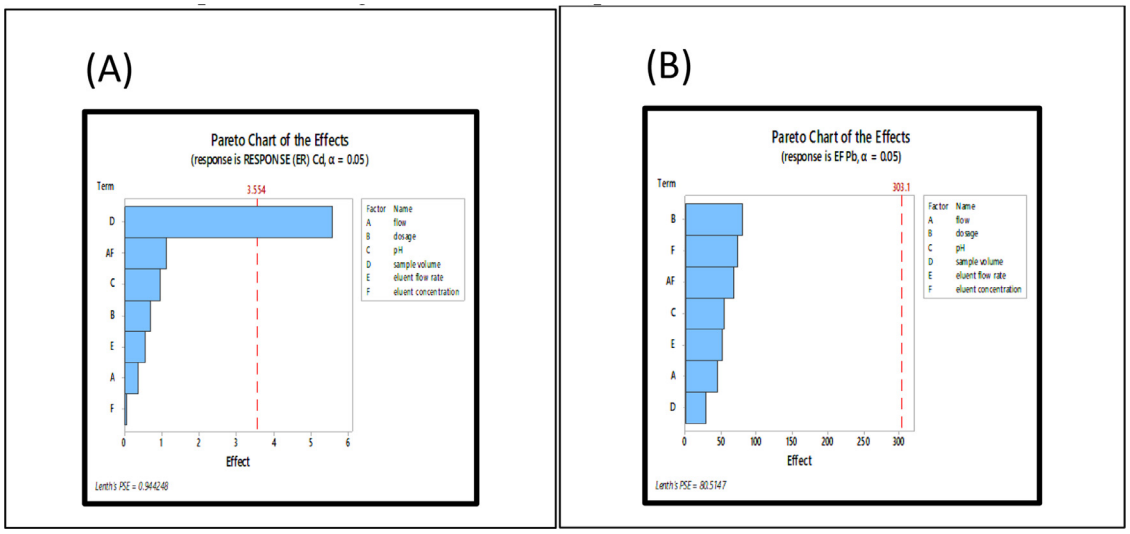

Fig. 3. Pareto chart for the effects on flow, dosage, pH, sample volume, eluent flow rate and eluent concentration on extraction recovery of (A)cadmium and (B) lead.

and sorption mechanism was mainly physical in nature. Lead fitted into the *Freundlich* isotherm model with $R = 0.975$ and represented by Eq. (4),

$$lnq_e = ln\,2.18 + \frac{1}{1.2lnC_e} \tag{4}$$

Screening of significant factors for cadmium *and* lead *extraction*

A Half factorial design, with 8 runs using Minitab 18 was used to screen for the significant variables which affect the removal efficiency of cadmium and lead from water. The optimized variables included sample flow rate, dosage, pH., sample volume, eluent flow rate and eluent concentration.

A Pareto chart, (Fig. 3) was used select the significant variables for cadmium recovery according to their estimated effects. Each variable which exceeded the reference line was considered to be significant at 95% confidence interval. The sample volume was found to be the most significant variable for cadmium recovery and the other variables were insignificant. The other factors were kept constant in subsequent experiments. In this case of lead, no variable was found to be significant at 95% confidence interval. Sample volume was significant for cadmium not lead because sample volume for cadmium experience most interactions with other factors such as pH and dosage whereas lead experience few interactions.

Optimization of the significant extraction conditions for cadmium *and* lead *using the Taguchi design*

Optimization of the significant variables was carried out using the Taguchi experimental design and included 16 runs in order to determine the varied variables which are sample volume, dosage, and pH and eluent concentration. The model to predict the enrichment factor of cadmium and lead is shown in Eq. (5) & (6) respectively. A positive value indicates enhancement and a negative value vice versa.

$$\begin{aligned}\text{EF cadmium} = {} & -1.59 + 0.0435\ \text{V} - 0.0249\ \text{D} + 1.115\ \text{P} + 0.000432\ \text{V2} + 0.000109\ \text{D2} \\ & - 0.0989\ \text{P2} - 0.000287\ \text{VD} - 0.00438\ \text{VP} + 0.00175\ \text{DP}\end{aligned} \tag{5}$$

$$\begin{aligned}\text{EF lead} = {} & 14.1 + 0.395\,V + 0.019\,D - 4.94\,P + 0.00382\ \text{V2} + 0.000055\ \text{D2} + 0.555\ \text{P2} \\ & - 0.00223\ \text{VD} - 0.0908\ \text{VP} + 0.0085\ \text{DP}\end{aligned} \tag{6}$$

Where V is sample volume, D is sorbent dosage, P is pH of the solution.

Evaluation of significant factors and interactions using analysis of variance (ANOVA)

In order to test the probable interactions between variables and important effects , ANOVA was carried out using Minitab 18 and the probability values less than 5% indicated statistical significance at 95% confidence level. In this case the linear model and sample volume were statistically significant parameters. The coefficient of determination (R^2) for the model is

Table 1
Anova table for the Taguchi model for optimization of enrichment of lead from water samples.

Source	DF	Adj SS	Adj MS	F-Value	P-Value
Model	9	906.18	100.687	1.48	0.327
Linear	3	220.96	73.655	1.08	0.426
sample volume	1	55.89	55.893	0.82	0.400
dosage	1	18.22	18.219	0.27	0.624
pH	1	115.24	115.236	1.69	0.241
sample volume*sample volume	1	137.45	137.446	2.02	0.205
dosage*dosage	1	0.22	0.215	0.00	0.957
2-Way Interaction	3	215.37	71.791	1.05	0.435
sample volume*dosage	1	67.41	67.408	0.99	0.358
sample volume*pH	1	204.83	204.827	3.01	0.134
dosage*pH	1	4.91	4.908	0.07	0.797
S	R-sq.	R-sq.(ad)	R-sq. (predicted)		
8.25452	68.91	22.28%	0.00%		

Table 2
Anova table for the Taguchi model for optimization of enrichment of cadmium from water samples.

Source		DF	Seq SS	Contribution	Adj SS	Adj MS	F-Value	P-Value
Model		9	37.46	0.92	37.46	4.16	7.26	0.013
Linear		3	30.12	0.74	14.00	4.67	8.14	0.016
sample volume		1	28.80	0.70	11.30	11.30	19.71	0.004
dosage		1	1.14	0.03	1.54	1.54	2.68	0.152
pH		1	0.19	0.00	0.51	0.51	0.90	0.38
Square		3	5.82	0.14	5.13	1.71	2.98	0.118
sample volume*sample volume		1	2.51	0.06	1.76	1.76	3.07	0.13
dosage*dosage		1	0.74	0.02	0.86	0.86	1.50	0.266
pH*pH		1	2.57	0.06	2.50	2.50	4.37	0.082
2-Way Interaction		3	1.52	0.04	1.52	0.51	0.88	0.501
sample volume*dosage		1	0.79	0.02	1.12	1.12	1.95	0.212
sample volume*pH		1	0.52	0.01	0.48	0.48	0.83	0.397
dosage*pH		1	0.21	0.01	0.21	0.21	0.36	0.57
Error		6	3.44	0.08	3.44	0.57		
Total		15	40.90	1.00				
S	**R-sq.**	R-sq.(adjusted)		PRESS		R-sq.(predicted)		
0.757152	**91.59%**	78.97%		42.478		0.00%		

0.9159 implying the model can explain 91.59% of the observed variation in the experimental results by changing variables of the modelled parameters. ANOVA was used to test the significance of the Taguchi design model for lead and cadmium and the the results are presented in Table 1 and 2 respectively. In the case for the enrichment of lead, the values of p were above 5% at 95% confidence interval meaning that they were not statistically significant at selected variables. Hence enrichment of lead is independent of any change in variables and can be carried out under any conditions. However, for the enrichment of cadmium, the effect of the sample volume was statistically significant as well as the model itself.

Main effects of sample volume, dosage and pH on the enrichment of cadmium *and* lead *using* $P-ZrO_2CeO_2ZnO$ *nanoparticles/alginate*

The sample volume is an important parameter in enrichment studies since high enrichment factors are desirable when analysing trace metals in real samples. There was an exponential increase in enrichment factor for cadmium (Fig 4a) when sample volume changed from its lowest level to its highest level assuming all other factors were kept constant. There was a decrease at first followed by an increase in enrichment factor for lead (Fig 4b) when sample volume changed from its low to its high level assuming all other factors were kept constant. The use of a large sample volume allowed for the enrichment factor to be improved in this case; hence the 100 mL sample volume was selected as the optimum in this study. Further higher volumes were avoided since they require larger amounts of adsorbents and requires more eluent and elution time for desorption.

There was a decrease in enrichment factor for lead and cadmium when the sorbent dosage changed from its low level to its high level when all other factors were kept constant. When the amount of adsorbent increases in solid phase extraction experiments desorption of the analytes attached to the adsorbent becomes difficult and therefore it is necessary to use a higher eluent volume which results in a decrease in sensitivity and extraction efficiency [40]. The extraction efficiency does not increase with an increase in dosage because the concentration of the metal ions are kept constant [45].

A gradual increase in enrichment factor for cadmium under acidic conditions followed by a decrease from pH 6 was observed when pH changed from pH 3.0 to 9.0 when all the other factors were kept constant was observed. There was a decrease in enrichment factor for lead when pH changes from pH 3.0–9.0 when all other factors were kept constant.

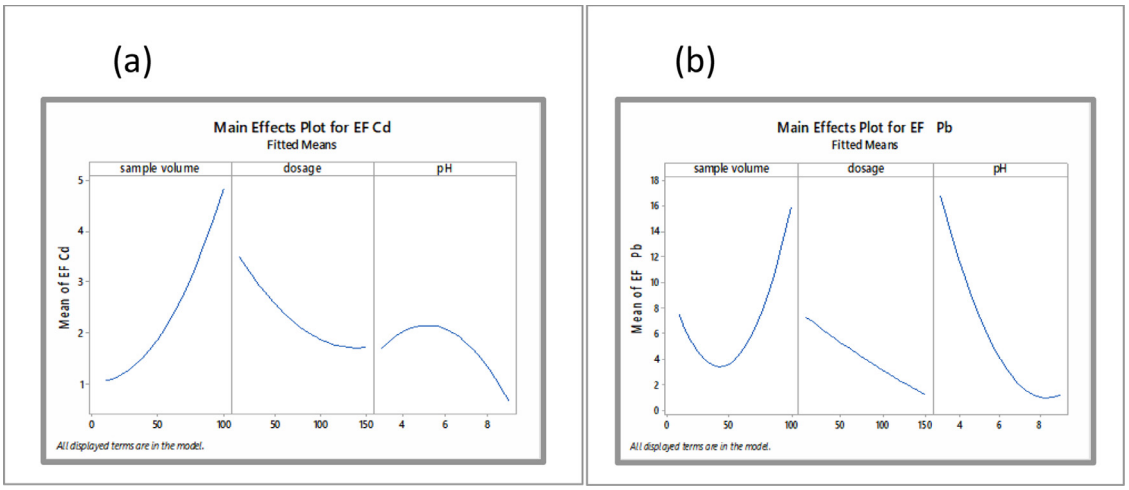

Fig. 4. The main effect of sample volume, dosage and pH on the enrichment factor of (A) cadmium and (B) lead.

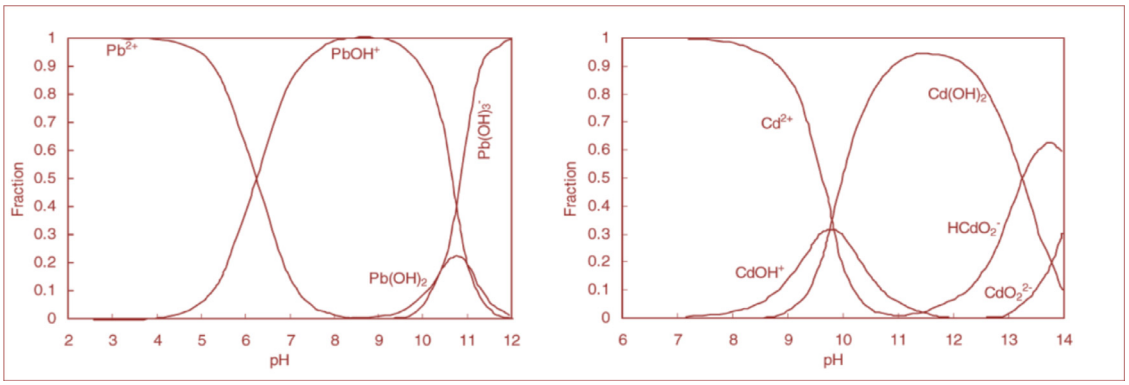

Fig. 5. Distribution of lead hydroxide and cadmium hydroxide at various pH.

Sorption of lead was found to be high at low pH. The uptake of the metal ions was affected by which ions is sorbed at a particular pH as shown in Fig. 5, hence in this case the lead (II) was the dominating ion for lead. In basic solution hydroxide ions may form complexes with the metal ions and precipitate them whereas in acidic solutions protonation of binding sites of chelating molecules may also occur thereby affecting the enrichment of the lead and cadmium [41].

Optimum conditions were obtained using the Half factorial design and the levels which produced the highest enrichment factors with few interactions were selected as the optimum conditions

Evaluation of the most significant factors and interactions using response surface, methodology and interaction plots

The enrichment factor increased with enhancing sample volumes whereas an increase in sorbent dosage resulted in a decline in enrichment "factor," and this was due to the sample reaching equilibrium earlier as shown in surface plots in Fig. 6. The enrichment factor was enhanced when an increase in sample volume from 5 to 100 mL was carried out. When pH was increased for the same experiment, the enrichment factor decreased due to analytes and surface properties of sorbent being affected such that they favour or hinder sorption, as shown in surface plots in Fig. 6. When the adsorbent dosage was increased from 50 mg to 150 mg, it resulted in a decrease in enrichment factor due to the early attainment of equilibrium. An increase in pH resulted in enhanced enrichment factor up until neutral pH and the enrichment factor started to decline thereafter because the forms of analytes and sorbent surface chemistry changes as pH changes favouring either uptake or inhibition.

Interactions occurred between sample volume and dosage as shown in Fig. 7. Interactions were observed at sample volume below 30 mL for both cadmium (Fig. 7a) and lead (Fig. 7g). Interactions were also experienced for dosages above 80 mg for cadmium (Fig. 7c) whereas for lead they were observed below 40 mg and above 100 mg (Fig. 7i). Interaction occurred between sample volume and pH for sample volume less than 30 mL and above 70 mL for cadmium (Fig. 7b); and only below 50 mL for lead (Fig. 7h). Interactions were also observed below pH 5 and above pH 7 for lead (Fig. 7k). Interactions were observed for dosage below 50 mg for cadmium (Fig. 7b) and above pH 7 for cadmium (Fig. 7f).

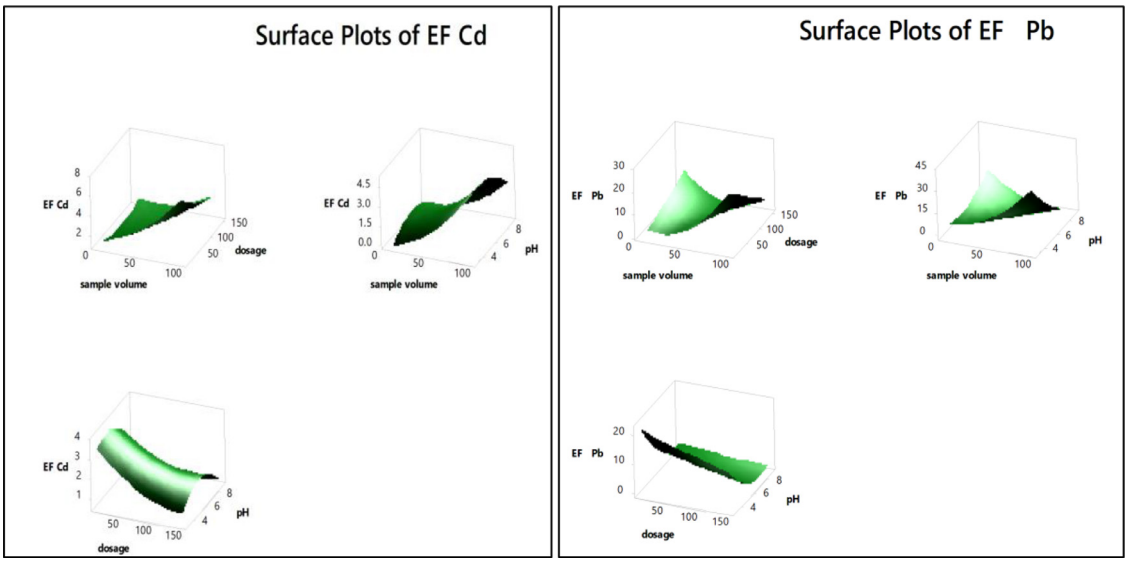

Fig. 6. The surface plots for sample volume, dosage and pH against enrichment factor of A) lead and B) cadmium.

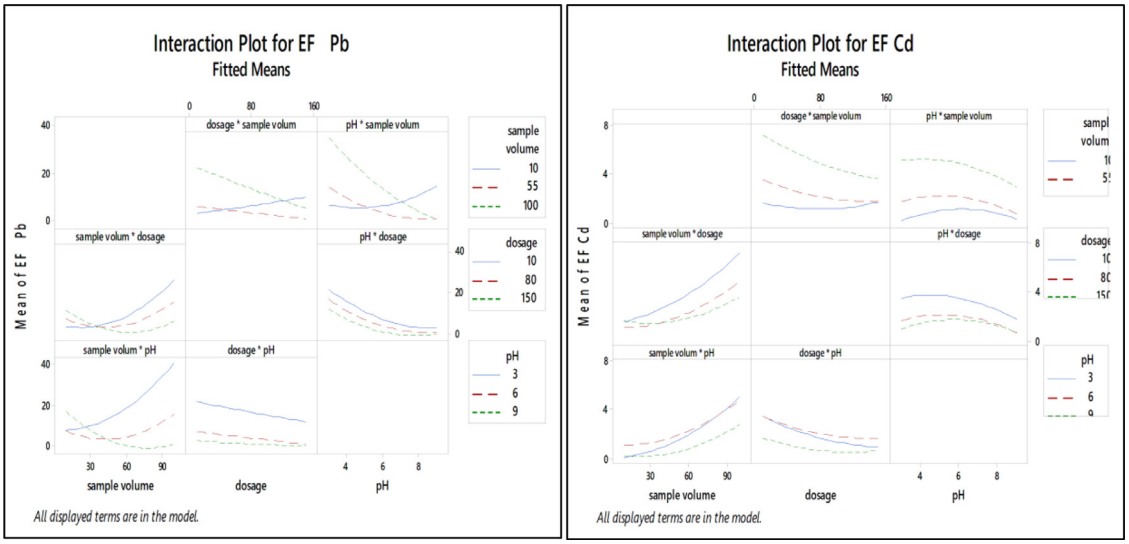

Fig. 7. The "Interaction plots," for sample volume, dosage and pH against enrichment factor for lead and cadmium.

Effect of 1%, 5% and 10% phenol and propan-2-ol on recovery of lead and cadmium

Metals and other coexisting ions associated with heavy metals show interferences in the presence of some heavy metal ions. The interferences occurs as the metal ions participates in redox reactions, formation of precipitates and complexation reactions [1]. The effect of anions and metals have been investigated by several authors and results show that metals interactions are mainly antagonistic [26]. The effect of organic contaminants has been rarely investigated hence in this study the effect of alcohols on recoveries of cadmium and lead metals was determined by varying the concentration from 1%, 5%, 10% phenol and propan-2-ol at pH 7, sorbent dosage 50 mg and 10 µg/L cadmium and lead concentration and the results are shown in Fig. 8. Phenol enhances cadmium and lead recovery at low concentrations up to 5% and depresses recovery at high concentrations. Propanol enhances recovery at low concentrations and depresses recovery at 5 and 10%. High alcohols concentration depress recovery due to enhancement of bonding between sorbent and metal ion.

The desorption cycles for the recovery of cadmium and lead from water samples.

Five adsorption-desorption cycles were carried out in order to assess the effectiveness of the sorbent to recover cadmium and lead from water samples as shown in Fig. 9. The extraction recovery of cadmium and lead are almost constant for 4

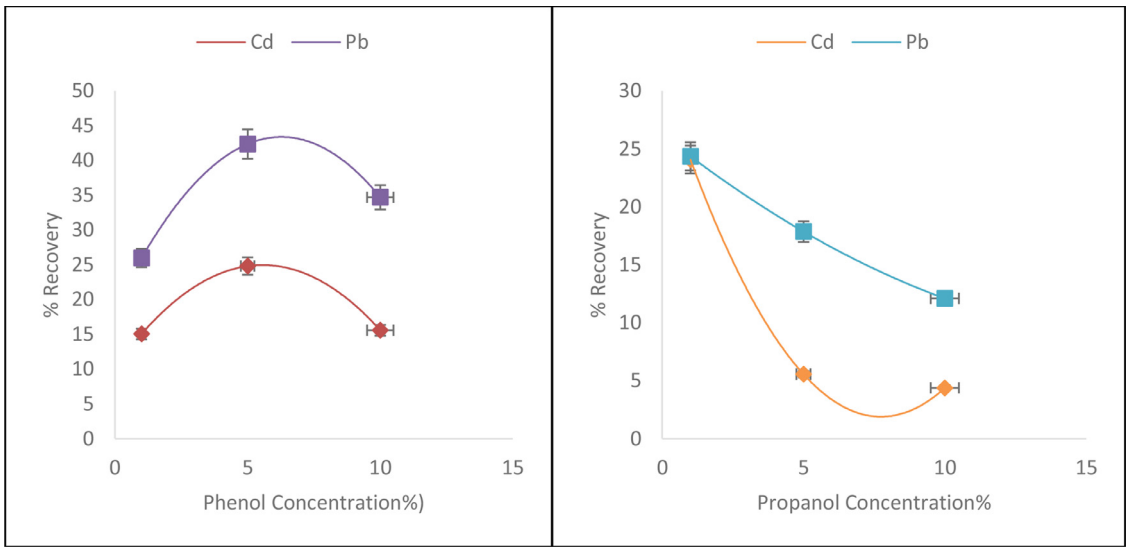

Fig. 8. The effect of increasing the concentration of phenol and propanol on recoveries of cadmium and lead from water samples.

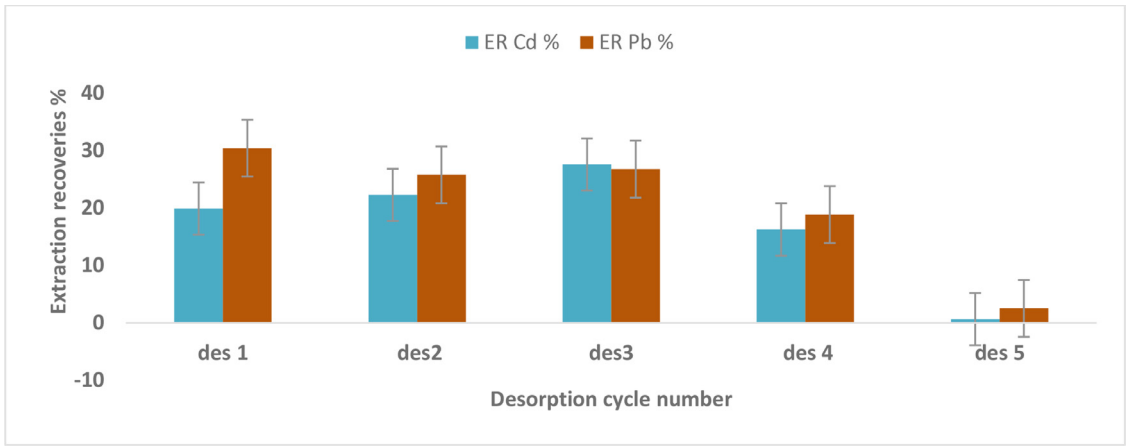

Fig. 9. cadmium and lead adsorption desorption cycles.

cycles however it is depressed at the 5th cycle. The lower recovery values may be due to strong adsorption which hinders the desorption step leading to a decrease in the recovery values [27].

Analytical performance

Six calibration standards ranging from 0 - 1,000,000 ng/L were used to determine the linearity of the method. The fit of the calibration points was determined using linear regression. Five extractions of 50,000 ng/L cadmium and lead water samples were used to determine method precision (repeatability) by calculating the relative standard deviation. The limit of detection (LOD) is defined as 3 Sb/m and the limit of quantification LOQ is defined as 10 Sb/m where Sb is the standard deviation of the blank signals and m is the slope of the calibration curve. The results of the acceptance criteria are shown in Table 3.

Analytical applications

The validation of the proposed procedure was determined by carrying out addition recovery experiments on real water samples and the results are shown in Table 4. It was done by spiking real samples from well and borehole water with metal ions and recoveries were calculated using Eq. (7). Spiking was done at three different "levels," namely 1.0, 5.0 and 10 µg/L for each metal ion. The borehole water sample was collected at in Avondale, Harare and the well water sample was collected

Table 3
Results of acceptance criteria for the analysis.

Parameter	Results	
	cadmium	lead
Range of linearity	0–1,000,000 ng/L	0–1,000,000 ng/L
LOD mg/L	0.0297 ng/L	0.1022 ng/L
LOQ mg/L	0.09902 ng/L	0.3407 ng/L
R^2	0.9978	0.9981
Precision	5.83	9.14
Recovery (ER)%	57.0 −147.70	33.12- 116.5

Table 4
Recoveries for well water and borehole water.

	Well water			*Borehole water*		
	Added µg/L	Found µg/L	Recovery%	Added µg/L	Found µg/L	Recovery%
lead	0.00	−0.77±4.342		0.00	0.21±4.147	
	1.00	0.08±0.315	8.0	1.00	0.98±1.071	77.01
	5.00	0.88±0.116	17.6	5.00	4.59±0.234	87.6
	10.00	10.88±1.922	108.0	10.00	7.88±1.3115	76.7
cadmium	0.00	0.29±2.09		0.00	1.46±1.269	
	1.00	2.22±0.314	193.0	1.00	2.03±0.655	57
	5.00	6.01±0.084	114.4	5.00	4.25±0.311	55.73
	10.00	15.06±0.905	147.70	10.00	11.82±0.305	103.55

Table 5
The comparison the presented enrichment study with some previously published enrichment studies.

Sorbent	*Metal ions*	*Determinationmethod*	*LOD*	*Precision%*	*Recovery (%)*	*REF*
$P-ZrO_2CeO_2ZnO$ ***nanoparticles @ alginate beads***	cadmium lead	ICP-MS	0.03 ng/L 0.102 ng/L	5.83 9.14	57.0–147.7 33.12–116.5	This study
3D-printed column with porous PA6 monolithic packing	manganese, cobalt, copper, zinc, cadmium and lead	ICP-MS	0.2–7.7 ng/L		94.3–98.5	[5]
Iminoacetate	cadmium lead	ICP-MS	2.7 pM 1.5 pM	4.1 5.5	92.2 97.6	[33]
Fe_3O_4@SiO_2@PCN-224 ***(MPCN-224)***	lead, zinc, chromium, bismuth	ICP-MS	0.94–11.4 ng/L		84.0–110	[43]
Hyper branched grapheme oxide immobilized polystyrene spherical sorbents	cadmium lead	ICP-OES	1.8 ng/L 1.5 ng/L	<5	98–104	[1]
Fe_3O_4@SiO_2	cadmium lead	FAAS	 0.05 ng/ml 0.9 ng/ml	5.8 6.0	95–104	[38]
Thermophilic bacteria *"Geobacillus galactosidasius,"* loaded on magnetic nanoparticles	cadmium lead	ICP-OES	 0.06 ng/ml 0.07 ng/ml	3.8 2.8	94.9 95.6	[34]

from Retreat farm in Waterfalls.

$$\text{Recovery } \% = \frac{C_s - C_0}{s} \quad (7)$$

where "C_s," concentration of analyte in the spiked sample, " C_0," concentration of metal ions in the unspiked water sample and "*s*," is amount of standard spiked.

Comparison with other methods

The analytical performance of the method was compared with other reported methods as shown in Table 5 and it compares well in terms of very low LOD. However, the high values for precision of lead enrichment suggest that further work on the sorbent metal uptake properties is needed to improve its efficiency.

Conclusion

This study shows the feasibility of enrichment of cadmium and lead on $P-ZrO_2CeO_2ZnO$ nanoparticles/ alginate beads prior to ICP-MS determination. The synthesized beads were amorphous in nature. Cadmium uptake followed the Dubinin Radushkevich isotherm model and Pb uptake followed the Freundlich isotherm model. The significant variable for cadmium enrichment at 95 % confidence interval was sample volume. The optimum conditions for enrichment of cadmium and lead were sample volume was 100 mL and pH 4. Phenol enhanced cadmium and lead enrichment at low concentrations up to 5% and at high concentrations it depressed enrichment. High sample volume, low sorbent dosage and acidic pH favoured enrichment of both cadmium and lead. The obtained LOD was comparable with other methods from literature. The range of linearity was between 0 and 1,000,000 ng/L, limits of detections were 0.027 and 0.1022 ng/L for cadmium and lead respectively, precisions were 5.83% and 9.14% for cadmium and lead respectively. The beads show great potential for use during enrichment of cadmium and lead from water.

Declaration of Competing Interest

The authors declare that they have no known competing financial interests or personal relationships that could have appeared to influence the work reported in this paper.

Acknowledgement

The authors would like to acknowledge Bindura University of Science Education and Government Analyst Laboratory for supply of chemicals and equipment.

References

[1] H. Ahmad, C. Cai, C. Liu, Separation and preconcentration of Pb(II) and Cd(II) from aqueous samples using hyperbranched polyethyleneimine-functionalized graphene oxide-immobilized polystyrene spherical adsorbents, Microchem. J. 145 (2019) 833–842, doi:10.1016/j.microc.2018.11.032.
[2] A. Azari, M. Yeganeh, M. Gholami, M. Salari, The superior adsorption capacity of 2,4-Dinitrophenol under ultrasound-assisted magnetic adsorption system: modeling and process optimization by central composite design, J. Hazard. Mater. 418 (2021) 126348, doi:10.1016/j.jhazmat.2021.126348.
[3] M.Y. Badi, A. Esrafili, H. Pasalari, R.R. Kalantary, E. Ahmadi, M. Gholami, A. Azari, Degradation of dimethyl phthalate using persulfate activated by UV and ferrous ions: optimizing operational parameters mechanism and pathway, J. Environ. Health Sci. Eng. 17 (2019) 685–700, doi:10.1007/s40201-019-00384-9.
[4] M. Baghayeri, H. Alinezhad, M. Fayazi, M. Tarahomi, R. Ghanei-Motlagh, B. Maleki, A novel electrochemical sensor based on a glassy carbon electrode modified with dendrimer functionalized magnetic graphene oxide for simultaneous determination of trace Pb(II)and Cd(II), Electrochim. Acta 312 (2019) 80–88, doi:10.1016/j.electacta.2019.04.180.
[5] Jyun Ran Chen, Jing Ru Chen, C.K. Su, Solution Foaming–Treated 3D-Printed monolithic packing for enhanced solid phase extraction of trace metals, Talanta 241 (2022) 123237, doi:10.1016/j.talanta.2022.123237.
[6] M. Darroudi, S.J. Hoseini, R. Kazemi Oskuee, H.A. Hosseini, L. Gholami, S. Gerayli, Food-directed synthesis of cerium oxide nanoparticles and their neurotoxicity effects, Ceram. Int. 40 (2014) 7425–7430, doi:10.1016/j.ceramint.2013.12.089.
[7] F. Davar, A. Majedi, A. Mirzaei, Polyvinyl alcohol thin fi lm reinforced by green synthesized zirconia nanoparticles, Ceram. Int. 44 (2018) 19377–19382, doi:10.1016/j.ceramint.2018.07.167.
[8] A.H. El-Sheikh, F.S. Nofal, M.H. Shtaiwi, Adsorption and magnetic solid-phase extraction of cadmium and lead using magnetite modified with schiff bases, J. Environ. Chem. Eng. 7 (2019) 103229, doi:10.1016/j.jece.2019.103229.
[9] M. Fayazi, M.A. Taher, D. Afzali, A. Mostafavi, M. Ghanei-Motlagh, Synthesis and application of novel ion-imprinted polymer coated magnetic multi-walled carbon nanotubes for selective solid phase extraction of lead(II) ions, Mater. Sci. Eng. C 60 (2016) 365–373, doi:10.1016/j.msec.2015.11.060.
[10] P. Geetha, M.S. Latha, S.S. Pillai, B. Deepa, K. Santhosh Kumar, M. Koshy, Green synthesis and characterization of alginate nanoparticles and its role as a biosorbent for Cr(VI) ions, J. Mol. Struct. 1105 (2016) 54–60, doi:10.1016/j.molstruc.2015.10.022.
[11] M. Ghorbani, M. Aghamohammadhassan, H. Ghorbani, A. Zabihi, Trends in sorbent development for dispersive micro-solid phase extraction, Microchem. J. 158 (2020) 105250, doi:10.1016/j.microc.2020.105250.
[12] K. Greda, M. Gorska, M. Welna, P. Jamroz, P. Pohl, In-situ generation of Ag, Cd, Hg, In, Pb, Tl and Zn volatile species by flowing liquid anode atmospheric pressure glow discharge operated in gaseous jet mode – evaluation of excitation processes and analytical performance, Talanta 199 (2019) 107–115, doi:10.1016/j.talanta.2019.02.058.
[13] U.R. Gudla, B. Suryanarayana, V. Raghavendra, K.A. Emmanuel, N. Murali, P. Taddesse, D. Parajuli, K. Chandra Babu Naidu, Y. Ramakrishna, K. Chandramouli, Optical and luminescence properties of pure, iron-doped, and glucose capped ZnO nanoparticles, Res. Phys. 19 (2020) 103508, doi:10.1016/j.rinp.2020.103508.
[14] S. Habib, A. Hassanein, R. Kahraman, E. Mahdi Ahmed, R.A. Shakoor, Self-healing behavior of epoxy-based double-layer nanocomposite coatings modified with Zirconia nanoparticles, Mater. Des. 207 (2021) 109839, doi:10.1016/j.matdes.2021.109839.
[15] M. Háková, L. Chocholoušová Havlíková, P. Solich, F. Švec, D. Šatínský, Electrospun nanofiber polymers as extraction phases in analytical chemistry – The advances of the last decade, TrAC 110 (2019) 81–96, doi:10.1016/j.trac.2018.10.030.
[16] M. He, L. Huang, B. Zhao, B. Chen, B. Hu, Advanced functional materials in solid phase extraction for ICP-MS determination of trace elements and their species - A review, Anal. Chim. Acta 973 (2017) 1–24, doi:10.1016/j.aca.2017.03.047.
[17] N. Hokonya, C. Mahamadi, synthesis of micro-particles using hydrocotyle ranunculoides (floating water pennywort) and their use in cadmium adsorption, IOSR J. Appl. Chem. 10 (2017) 14–23, doi:10.9790/5736-1005021423.
[18] S. Illuminati, A. Annibaldi, C. Truzzi, G. Libani, C. Mantini, G. Scarponi, Determination of water-soluble, acid-extractable and inert fractions of Cd, Pb and Cu in Antarctic aerosol by square wave anodic stripping voltammetry after sequential extraction and microwave digestion, J. Electroanal. Chem. 755 (2015) 182–196, doi:10.1016/j.jelechem.2015.07.023.
[19] J. Jayadevimanoranjitham, S. Sriman Narayanan, A mercury free electrode based on poly O-cresophthalein complexone film matrixed MWCNTs modified electrode for simultaneous detection of Pb (II) and Cd (II), Microchem. J. 148 (2019) 92–101, doi:10.1016/j.microc.2019.04.029.
[20] K.S. Joshy, M.A. Susan, S. Snigdha, K. Nandakumar, A.P. Laly, T. Sabu, Encapsulation of zidovudine in PF-68 coated alginate conjugate nanoparticles for anti-HIV drug delivery, Int. J. Biol. Macromol. 107 (2018) 929–937, doi:10.1016/j.ijbiomac.2017.09.078.
[21] H. Karami, N. Shariatifar, S. Nazmara, M. Moazzen, B. Mahmoodi, A. Mousavi Khaneghah, the concentration and probabilistic health risk of potentially toxic elements (PTEs) in edible mushrooms (wild and cultivated) samples collected from different cities of Iran, Biol. Trace Elem. Res. (2020) 389–400, doi:10.1007/s12011-020-02130-x.

[22] M. Karimi, S. Dadfarnia, A.M.H. Shabani, F. Tamaddon, D. Azadi, Deep eutectic liquid organic salt as a new solvent for liquid-phase microextraction and its application in ligandless extraction and preconcentraion of lead and cadmium in edible oils, Talanta 144 (2015) 648–654, doi:10.1016/j.talanta.2015.07.021.
[23] N.A. Kasa, S. Sel, D.S. Chormey, S. Bakırdere, Determination of cadmium at trace levels in parsley samples by slotted quartz tube-flame atomic absorption spectrometry after preconcentration with cloud point extraction, Measurement 147 (2019) 106841, doi:10.1016/j.measurement.2019.07.069.
[24] S.A. Kitte, S. Li, A. Nsabimana, W. Gao, J. Lai, Z. Liu, G. Xu, Stainless steel electrode for simultaneous stripping analysis of Cd(II), Pb(II), Cu(II) and Hg(II), Talanta 191 (2019) 485–490, doi:10.1016/j.talanta.2018.08.066.
[25] M. Krawczyk, M. Jeszka-skowron, Multiwalled carbon nanotubes as solid sorbent in dispersive micro solid-phase extraction for the sequential determination of cadmium and lead in water samples, Microchem. J. 126 (2016) 296–301, doi:10.1016/j.microc.2015.12.027.
[26] C. Mahamadi, B. Madocha, Adsorptive removal of Ni(II) from water using alginate-fixed water hyacinth: effect of organic substances, Am. J. Anal. Chem. 04 (2013) 373–378, doi:10.4236/ajac.2013.48047.
[27] G.J. Maranata, N.O. Surya, A.N. Hasanah, Optimising factors affecting solid phase extraction performances of molecular imprinted polymer as recent sample preparation technique, Heliyon 7 (2021) e05934, doi:10.1016/j.heliyon.2021.e05934.
[28] S. Millour, L. Noël, A. Kadar, R. Chekri, C. Vastel, T. Guérin, Simultaneous analysis of 21 elements in foodstuffs by ICP-MS after closed-vessel microwave digestion: method validation, J. Food Composit. Anal. 24 (2011) 111–120, doi:10.1016/j.jfca.2010.04.002.
[29] M. Mohebbi, R. Heydari, M. Ramezani, Determination of Cu, Cd, Ni, Pb and Zn in edible oils using reversed-phase ultrasonic assisted liquid–liquid microextraction and flame atomic absorption spectrometry, J. Anal. Chem. 73 (2018) 30–35, doi:10.1134/S1061934818010069.
[30] M. Monier, A.L. Shafik, D.A. Abdel-Latif, Surface molecularly imprinted amino-functionalized alginate microspheres for enantio-selective extraction of L-ascorbic acid, Carbohydr. Polym. 195 (2018) 652–661, doi:10.1016/j.carbpol.2018.04.106.
[31] S. Nekouei, F. Nekouei, I. Tyagi, S. Agarwal, V.K. Gupta, Mixed cloud point/solid phase extraction of lead(II) and cadmium(II) in water samples using modified-ZnO nanopowders, Process Saf. Environ. Protect. 99 (2016) 175–185, doi:10.1016/j.psep.2015.11.005.
[32] P.N. Nomngongo, J.C. Ngila, Multivariate optimization of dual-bed solid phase extraction for preconcentration of Ag, Al, As and Cr in gasoline prior to inductively coupled plasma optical emission spectrometric determination, Fuel 139 (2015) 285–291, doi:10.1016/j.fuel.2014.08.046.
[33] J.E. O'Sullivan, R.J. Watson, E.C.V. Butler, An ICP-MS procedure to determine Cd, Co, Cu, Ni, Pb and Zn in oceanic waters using in-line flow-injection with solid-phase extraction for preconcentration, Talanta 115 (2013) 999–1010, doi:10.1016/j.talanta.2013.06.054.
[34] S. Özdemir, E. Kilinç, V. Okumuş, A. Poli, B. Nicolaus, I. Romano, Thermophilic Geobacillus galactosidasius sp. nov. loaded γ-Fe2O3 magnetic nanoparticle for the preconcentrations of Pb and Cd, Bioresour. Technol. 201 (2016) 269–275, doi:10.1016/j.biortech.2015.11.052.
[35] G. Özzeybek, İ. Şahin, S. Erarpat, S. Bakirdere, Reverse phase dispersive liquid–liquid microextraction coupled to slotted quartz tube flame atomic absorption spectrometry as a new analytical strategy for trace determination of cadmium in fish and olive oil samples, J. Food Composit. Anal. 90 (2020), doi:10.1016/j.jfca.2020.103486.
[36] M. Rashidipour, R. Heydari, A. Feizbakhsh, P. Hashemi, Rapid monitoring of carvacrol in plants and herbal medicines using matrix solid-phase dispersion and gas chromatography flame ionisation detector, Nat. Prod. Res. 29 (2015) 621–627, doi:10.1080/14786419.2014.980247.
[37] J. Sardans, F. Montes, J. Peñuelas, Determination of As, Cd, Cu, Hg and Pb in biological samples by modern electrothermal atomic absorption spectrometry, Spectrochim. Acta Part B 65 (2010) 97–112, doi:10.1016/j.sab.2009.11.009.
[38] A. Tadjarodi, A. Abbaszadeh, M. Taghizadeh, N. Shekari, A.A. Asgharinezhad, Solid phase extraction of Cd(II) and Pb(II) ions based on a novel functionalized Fe3O4@ SiO2 core-shell nanoparticles with the aid of multivariate optimization methodology, Mater. Sci. Eng. C 49 (2015) 416–421, doi:10.1016/j.msec.2015.01.013.
[39] R. Tovar-Gómez, MdelR Moreno-Virgen, J. Moreno-Pérez, A. Bonilla-Petriciolet, V. Hernández-Montoya, C.J. Durán-Valle, Analysis of synergistic and antagonistic adsorption of heavy metals and acid blue 25 on activated carbon from ternary systems, Chem. Eng. Des. 93 (2015) 755–772, doi:10.1016/j.cherd.2014.07.012.
[40] H.İ. Ulusoy, E. Yılmaz, M. Soylak, Magnetic solid phase extraction of trace paracetamol and caffeine in synthetic urine and wastewater samples by a using core shell hybrid material consisting of graphene oxide/multiwalled carbon nanotube/Fe3O4/SiO2, Microchem. J. 145 (2019) 843–851, doi:10.1016/j.microc.2018.11.056.
[41] S. Uruş, S. Purtaş, G. Ceyhan, F. Tümer, Solid phase extraction of Pb(II), Cu(II), Cd(II) and Cr(III) with syringe technique using novel silica-supported bis(diazoimine) ligands, Chem. Eng. J. 220 (2013) 420–430, doi:10.1016/j.cej.2013.01.037.
[42] WHOGuidelines for Drinking-water Quality 1, 2011.
[43] C. Xu, M. He, B. Chen, B. Hu, Magnetic porous coordination networks for preconcentration of various metal ions from environmental water followed by inductively coupled plasma mass spectrometry detection, Talanta 245 (2022) 123470, doi:10.1016/j.talanta.2022.123470.
[44] L. Yao, H. Liu, X. Wang, W. Xu, Y. Zhu, H. Wang, L. Pang, C. Lin, Ultrasound-assisted surfactant-enhanced emulsification microextraction using a magnetic ionic liquid coupled with micro-solid phase extraction for the determination of cadmium and lead in edible vegetable oils, Food Chem. 256 (2018) 212–218, doi:10.1016/j.foodchem.2018.02.132.
[45] Y. Yuan, Y. Wu, H. Wang, Y. Tong, X. Sheng, Y. Sun, X. Zhou, Q. Zhou, Simultaneous enrichment and determination of cadmium and mercury ions using magnetic PAMAM dendrimers as the adsorbents for magnetic solid phase extraction coupled with high performance liquid chromatography, J. Hazard. Mater. 386 (2020) 121658, doi:10.1016/j.jhazmat.2019.121658.
[46] N. Zhang, H. Peng, B. Hu, Light-induced pH change and its application to solid phase extraction of trace heavy metals by high-magnetization Fe3O4@SiO 2@TiO2 nanoparticles followed by inductively coupled plasma mass spectrometry detection, Talanta 94 (2012) 278–283, doi:10.1016/j.talanta.2012.03.040.
[47] W.S. Zhong, T. Ren, L.J. Zhao, Determination of Pb (Lead), Cd (Cadmium), Cr (Chromium), Cu (Copper), and Ni (Nickel) in Chinese tea with high-resolution continuum source graphite furnace atomic absorption spectrometry, J. Food Drug Anal. 24 (2016) 46–55, doi:10.1016/j.jfda.2015.04.010.